Supplement of Atmos. Chem. Phys., 24, 4289–4304, 2024
https://doi.org/10.5194/acp-24-4289-2024-supplement

Atmospheric Chemistry and Physics
Open Access
EGU

Supplement of

Contribution of cooking emissions to the urban volatile organic compounds in Las Vegas, NV

Matthew M. Coggon et al.

Correspondence to: Matthew M. Coggon (matthew.m.coggon@noaa.gov)

1. Supplemental Figures to the Main Text

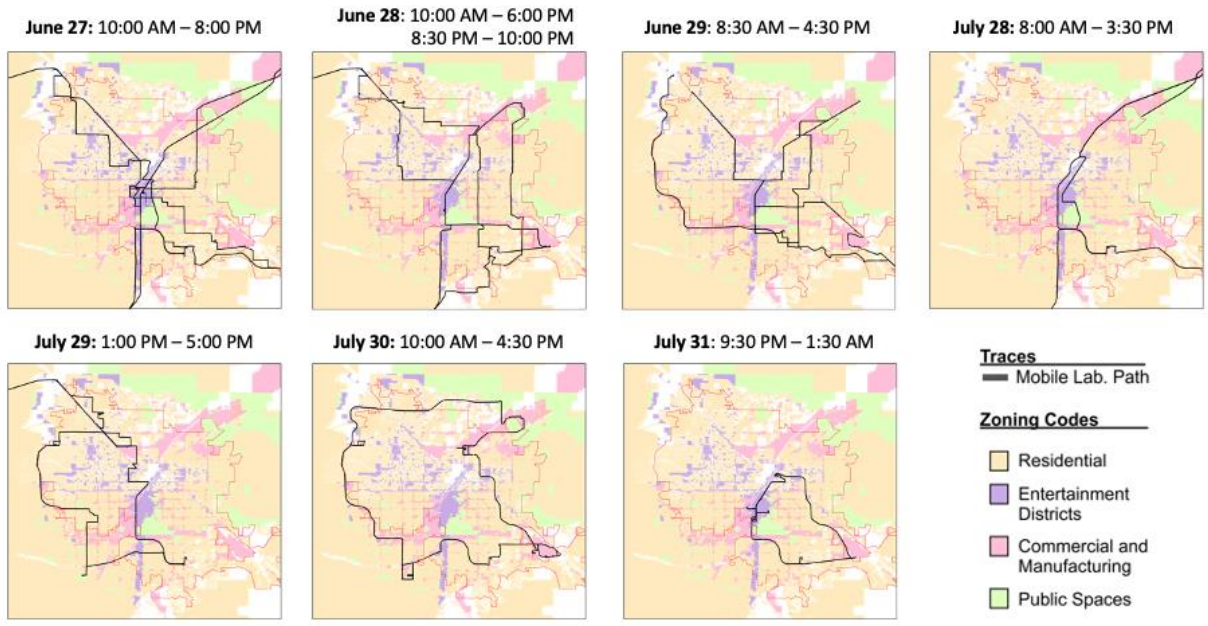

Figure S1: Daily mobile laboratory paths throughout Las Vegas and sampling times (in local time) for each of the drives.

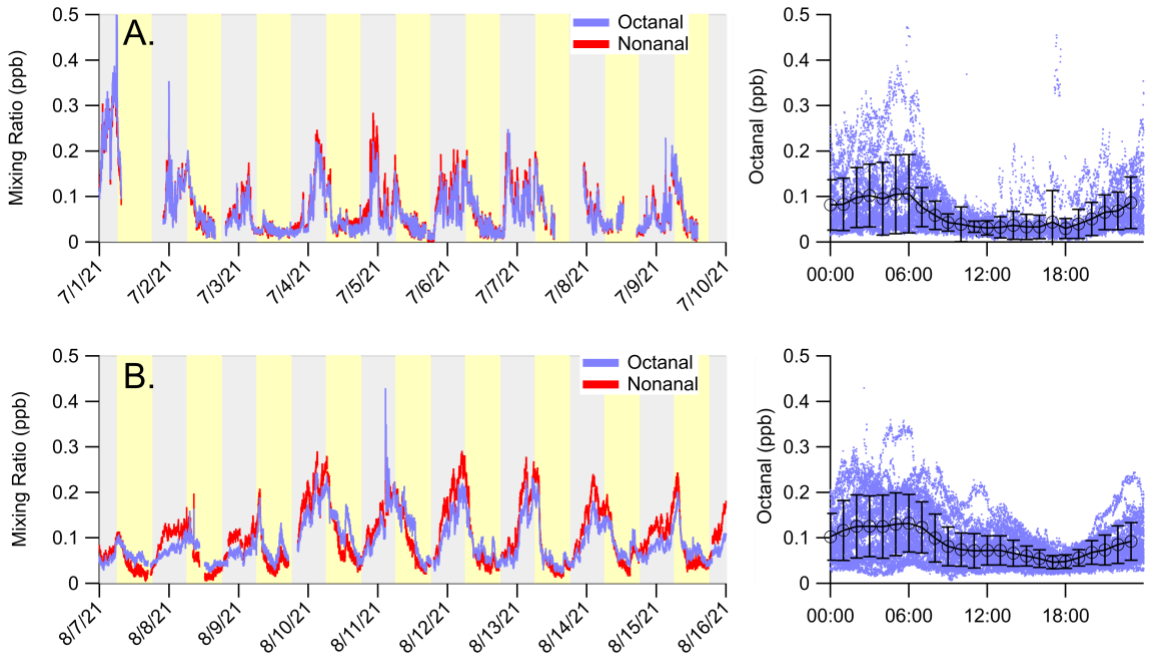

Figure S2: Time series and diurnal pattern of octanal and nonanal in (A) Las Vegas, NV and (B) Pasadena, CA. Yellow and grey backgrounds indicate measurements conducted during the day (6:00 AM – 6:00 PM local time) and night (6;00 PM – 6:00 AM), respectively.

2. Description of Restaurant Inspection Data

The South Nevada Health District (SNHD) maintains restaurant inspection reports for all commercial locations that sell food and beverages in Clark County, NV (SNHD, 2021). The full report includes inspections from 2005 – present. These reports are routinely updated and provide the locations, permit number, inspection grades, and inspection dates for each facility. Individual entries are categorized as restaurants, bars / taverns, markets, public facilities (e.g., schools), and other locations.

These data were accessed in December 2021 (~6 months from the completion of SUNVEx). The full record includes multiple entries for each permit holder. The data were first screened to retain only the most recent data for each permit. Next, the data were screened to only include facilities that were inspected after July 1, 2020 (i.e., one year before the SUNVEx campaign). This screening criteria reflects the minimum frequency that the SNHD conducts unannounced inspections. This criteria eliminates records that may be outdated or leftover from facilities that are no longer in operation. In this study, we present the locations of facilities categorized as restaurants, which represent 61% of the screened inspection reports (8,300 facilities). Snack bars (14%), bars / taverns (8%), food trucks (3%), school kitchens (3%), and less abundance facilities (11%) make up the remainder of the entries.

3. Characterizing PTR-ToF-MS Measurements of Carbonyls in Las Vegas

Long-chain carbonyls are measured by PTR-ToF-MS as the sum of isomers. Differences in isomer speciation provide evidence for varying emission sources. For example, VCP emissions from inks and coatings contain C_5 – C_7 ketones such as 2-heptanone and 4-methyl-2-pentanone (McDonald et al., 2018), while cooking emits high amounts of C_5 – C_7 aldehydes (Klein et al., 2016). VCPs emit few carbonyls with C > 7 (McDonald et al., 2018), whereas cooking is a significant source of C_8 – C_{11} aldehydes (Klein et al., 2016; Schauer et al., 1999). To determine the dominant carbonyls detected by PTR-ToF-MS in Las Vegas, GC-PTR-ToF-MS data are used to pre-separate isomers and evaluate carbonyl distributions.

Figure S3A is a GC-PTR-ToF-MS chromatogram of C_5 – C_9 carbonyls measured along the Las Vegas Strip during a nighttime drive on July 30, 2021. Each peak shows the expected proton-transfer reaction product (= VOC mass + H^+), the dehydration products that are typically observed from aliphatic aldehydes (= VOC mass + H^+ - H_2O) (Pagonis et al., 2019; Buhr et al., 2002), and additional ions that are expected from fragmentation for some molecules (e.g., octanal and nonanal). Figure S3B and S3C show chromatograms of C_8 and C_9 carbonyl standards as examples of how different carbonyls are detected by PTR-ToF-MS. The ketone isomers (e.g., 2-octanone and 2-nonanone) exhibit minimal fragmentation and are predominantly detected at the proton-transfer product at m/z 129 ($C_8H_{16}OH^+$) and m/z 143 ($C_9H_{18}OH^+$). In contrast, aldehydes mostly undergo dehydration and fragmentation, resulting in additional signals at m/z 111 ($C_8H_{15}^+$) and m/z 69 ($C_5H_8^+$) for octanal and 125 ($C_9H_{17}^+$), m/z 83 ($C_6H_{10}^+$), and m/z 69 ($C_5H_8^+$) for nonanal. Fragmentation patterns for other aldehydes are shown in Fig. S4 and compared to observations

from Buhr et al. (2002). The proton-transfer product for aldehydes increases with carbon number, while the contribution from the dehydration product deceases as additional fragmentation results in lower carbon ions. These differences in fragmentation distinguish ketone and aldehyde isomers in GC samples.

The GC-PTR-ToF-MS chromatograms in Figure S3A show that aldehydes are the dominant carbonyls observed in the Las Vegas Strip area. Broadly, the peaks show that the fragmentation patterns observed at major carbonyl retention times agree with the expected dehydration products of aldehydes. Closer inspection of the proton-transfer products show that signals from C_5 – C_7 ketone isomers are also present in this region (likely due to VCP emissions), and therefore the proton-transfer product ions for C_5 – C_7 carbonyls (m/z 115, 101, and 87) alone cannot provide robust constraints on the spatial and temporal distribution of aldehydes in urban areas. The dehydration products from C_5 – C_7 aldehydes (e.g., m/z 69, 83, and 97) distinguish these isomers from ketones, though it is unlikely that these ions could be used for aldehyde quantification since they are also produced from the proton-transfer of isoprene and fragmentation of cycloalkanes (Pagonis et al., 2019).

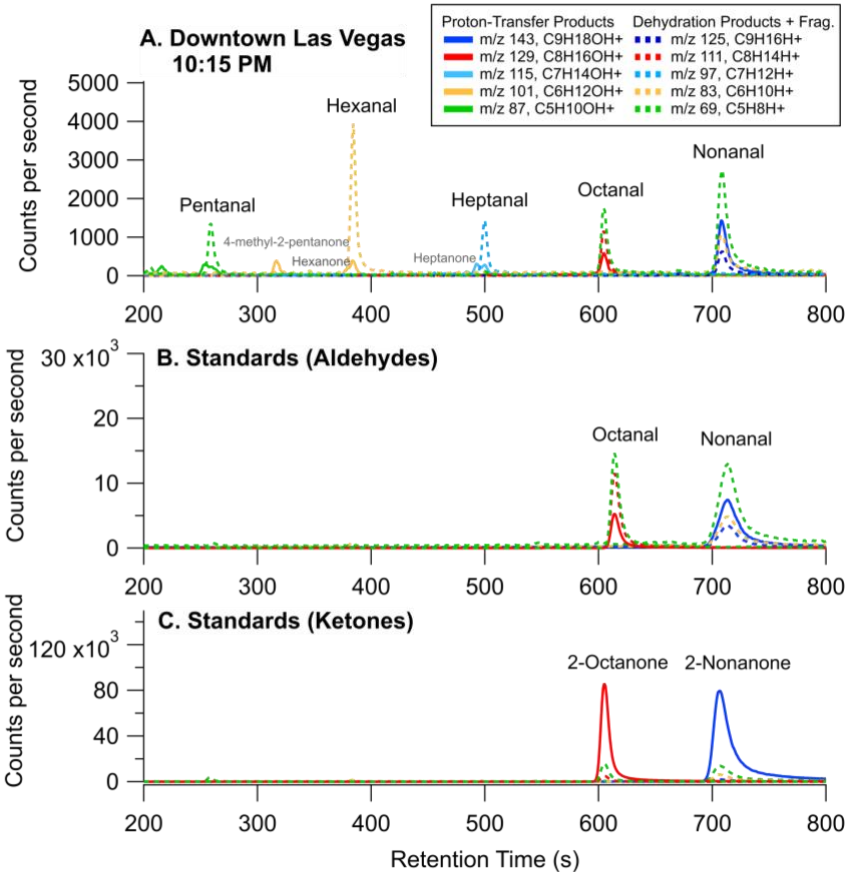

Figure S3: (A) GC-PTR-ToF-MS chromatogram showing aldehyde peaks in the Las Vegas Strip area during an evening drive on July 30, 2021. (B and C) GC-PTR-ToF-MS chromatogram of aldehyde and

ketone standards and their corresponding fragmentation patterns. The peaks in the ambient chromatogram correspond to aldehydes and not ketones.

Figure S3A shows that carbonyl proton-transfer products at m/z 129 and 143 do not exhibit significant contribution from ketones isomers in the Las Vegas Strip area. The ion distribution observed from the ambient GC-PTR-ToF-MS samples agrees well with the fragmentation patterns from octanal and nonanal standards (Fig. S3B), and no additional peaks are observed in the ambient chromatogram that would suggest significant contributions to these ions from other VOCs. Therefore, m/z 129 and m/z 143 can be used to quantify octanal and nonanal without significant interferences in the Las Vegas Strip area. The proton-transfer products for octanal and nonanal are also a larger fraction of the total signal compared to smaller aldehydes (Fig. S4), which indicates that these ions are detected with higher sensitivity.

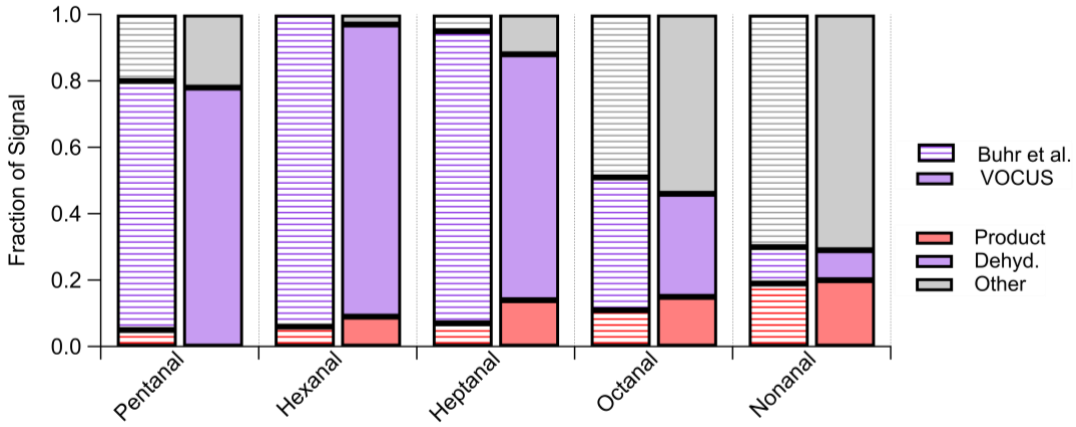

Figure S4: Distribution of ions detected by PTR-ToF-MS for C_5 – C_9 aldehydes. Solid bars represent distributions measured using a Vocus (this work) and hashed bars are distributions reported by Buhr et al. (Buhr et al., 2002). Contributions from "other" ions includes fragments and water clusters.

Mobile laboratory data also show that octanal and nonanal are the dominant carbonyl isomers throughout the Las Vegas region. Figure S3 shows PTR-ToF-MS measurements of m/z 129 and m/z 143 vs. dehydration products (m/z 125 and 111) for the entire mobile laboratory dataset. Other compounds, such as cycloalkanes, contribute to the signals at m/z 111 and 125 (Gueneron et al., 2015; Warneke et al., 2014), which explains periods when m/z 111 and 125 are elevated in the absence of m/z 129 and m/z 143. This also increases the variability in the dehydration products compared that observed for pure aldehyde standards. Most data scatter on a line that closely matches the expected fragmentation patterns for aldehydes (solid line). Furthermore, there are few data points that indicate significant contributions from ketones, which would be present as high contribution from proton-transfer products and low contributions from dehydration products (dotted line). Figures S3 and S5 demonstrate that the C_8 – C_9 carbonyls detected by PTR-ToF-MS in Las Vegas are predominantly associated with aldehydes.

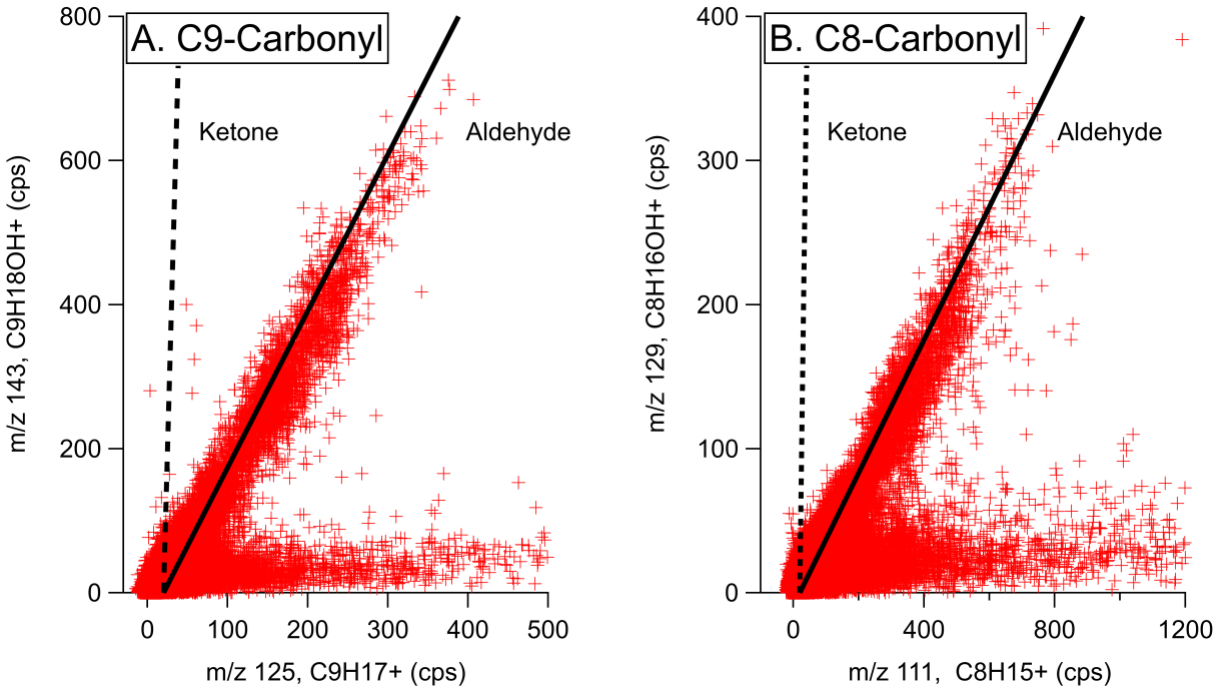

Figure S5: Mobile drive observations of (A) C_9 and (B) C_8 carbonyl proton-transfer products versus the corresponding dehydration products. The solid and dotted black lines show the aldehyde and ketone ratios from measured standards (Figure S3).

4. Corrections to Masses Identified as Aldehydes

Figure S4 shows that C_5-C_9 aldehydes undergo significant dehydration and fragmentation reactions in PTR-ToF-MS. These compounds are among the major VOCs emitted from cooking (Klein et al., 2016; Schauer et al., 1999); consequently, corrections to these species are needed to account for the mass associated with cooking emissions. In all figures and tables, we correct aldehyde sensitivities using the carbon-dependent fragmentation patterns shown in Fig. S4. First, we follow the methods described by Sekimoto et al. (2017) and determine PTR-ToF-MS sensitivities ($Sens_{est}$) using measured or estimated proton transfer rate constants. We then multiply this sensitivity by the fraction of total signal attributed to the proton-transfer rate constant of the aliphatic aldehyde with the same carbon number (α).

$$Sens_{Corr} = Sens_{est} \cdot \alpha$$

$$\alpha = \frac{S_{H3O}}{S_{H3O} + S_{Water\ Loss} + S_{Other}}$$

Where S_{H3O} is the signal associated with proton-transfer and $S_{Water\ Loss}$ and S_{other} are signals associated with water loss and other fragmentation processes. For aldehydes with C > 9, we assume α is similar to nonanal. We do not apply corrections to aldehydes with C < 5 since these compounds are not observed to fragment significantly in PTR-ToF-MS (Pagonis et al., 2019). Sensitivities for acetaldehyde, acrolein, propanal, methacrolein + crotonaldehyde, octanal, and nonanal are directly calibrated and therefore not corrected using this method.

5. Positive Matrix Factorization (PMF) Analysis

Positive matrix factorization (PMF) was conducted using the Source Finder (SoFi) software package in Igor Pro (Canonaco et al., 2013) to apportion VOCs to cooking and other urban emission sources, such as VCPs and motor vehicles. PMF is a bilinear factor model described by Paatero (1999) and its application to ambient mass spectra is widely used and summarized elsewhere (Canonaco et al., 2013; Ulbrich et al., 2009). In short, PMF statistically apportions a matrix of data (X) into the linear combination of factor profiles (G) and temporally varying factor abundancies (F) as described by Equation 1.

$$\mathrm{X} = \mathrm{GF} + \mathrm{E} \quad \text{(Eq 1)}$$

Where E is a matrix of model residuals. Inputs to the PMF algorithm include the time-varying data matrix, X, and a time-varying matrix of sample uncertainties (termed the "error matrix"). In this analysis, we evaluate the temporal behavior of 270 ions on a 10 min time basis. The error matrix reflects the uncertainty of each measurement and is calculated as two times the standard deviation of background mixing ratios.

The columns in G and the rows in F correspond to the "factors" fit by PMF to dataset X. Increasing the number of factors results in lower model residuals but can result in solutions that are non-physical. The number of factors fit to the dataset is partly chosen in order to minimize the model uncertainty to within measurement errors. The number of factors is also chosen in order to explain feasible emission sources and are justified by comparing factor profiles to molecular markers, emission fingerprints, or previously established factor profiles. In this analysis, PMF solutions were determined for 1–10 factors, but we focus on a PMF solution with 5 factors (see Section 2.2)

SoFi utilizes the multi-linear engine (ME-2) described by Paatero (1999). A key function of ME-2 is that it allows a user to input a factor profile that describes the relative distribution of VOCs associated with a given source. The degree to which this constraint is enforced in SoFi is dictated by a scalar "a-value" as described by Equation 2.

$$g_{i,solution} = g_i + a \cdot g_i \quad \text{(Eq 2)}$$

Where $g_{i,solution}$ is the factor solution resolved by PMF (G, Eq. 1), g_i is the factor profile constraint, and a is the a-value. When $a = 0$, $g_{i,solution}$ is fully constrained to g_i. Positive values allow the software to solve for $g_{i,solution}$ within uncertainty bounds dictated by the term $a \cdot g_i$. In this analysis, we constrain PMF with a mobile source profile derived from mobile measurements following the recommendations of Gkatzelis et al. (2021b) and vary a from 0.1–1 (See Section

2.1). A focus of this analysis are solutions where a = 0.75; however, we discuss how a 5-factor solution varies as a function of a (see Section 2.2).

5.1 Mobile Source Constraint

Previous PMF analyses on PTR-ToF-MS data in New York City (NYC) showed that resolving co-located sources can be challenging (Gkatzelis et al., 2021c). Fossil fuels were historically a dominant source of VOCs in US urban areas; however, years of regulation have resulted in major declines in fossil fuel VOC mixing ratios (Bishop and Haugen, 2018; Warneke et al., 2012). Consequently, molecules previously assigned to mobile sources, such as aromatics and ethanol, now have significant contributions from solvent sources such as paints and coatings (McDonald et al., 2018; Gkatzelis et al., 2021a; Gkatzelis et al., 2021c). For example, Figure S6 shows the time series of benzene, toluene, and the sum of C_8-aromatics measured at the Jerome Mack ground site. Benzene is often attributed to fossil fuels since it is banned from consumer products, while toluene and C_8-aromatics (e.g., xylenes) can result from both mobile sources and emissions from solvent-borne products (McDonald et al., 2018). At the Jerome Mack ground site, there are periods when aromatics correlate well (likely mobile source emissions), and there are periods when toluene and C_8-aromatics are significantly higher than benzene (likely due to a solvent source). Gkatzelis et al. (2021c) made similar observations in NYC, and it was found that an unconstrained PMF analysis resulted in a source apportionment that mixed the contributions from VCPs and mobile sources.

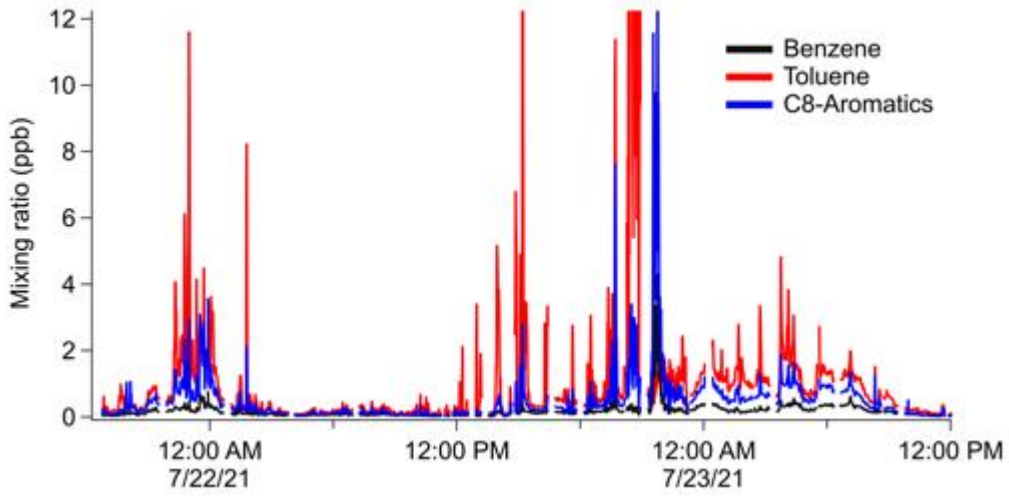

Figure S6. Time series of aromatic species measured at the Jerome Mack ground site.

To help separate mobile sources from VCPs in NYC, Gkatzelis et al. (2021c) constrained PMF with a mobile source profile that was representative of the fossil fuel emissions in the NYC area. This profile was determined using on-road VOC measurements measured by mobile laboratory, which can be used to identify and separate VOC plumes resulting from tailpipe emissions from other plumes resulting from sources such as VCPs. We follow the methods by Gkatzelis et al. (2021c) and determine a mobile source profile for Las Vegas using the mobile laboratory data collected throughout the Las Vegas Valley. Figure S7 illustrates our methods. Briefly, we identify periods when on-road mixing ratios of aromatic species, such as benzene, toluene, and C_8-aromatics, are enhanced above background mixing ratios by at least a factor of five (stringency criteria). We screen these plumes to exclude periods when VCP tracers are enhanced (e.g., monoterpenes, D5-siloxane). These on-road plumes must also be enriched in CO and NOx, which further differentiates mobile source enhancements of aromatics from solvent-borne emissions. We subtract out the local VOC background just outside of the plume to correct for VOCs with large regional mixing ratios (e.g., acetone, ethanol, etc.), then normalize plume-enhanced VOC mixing ratios by the total VOCs measured by PTR-ToF-MS. The mobile source profile is calculated as the average of these normalized plume profiles. In total, 100 plumes were identified and included in this analysis.

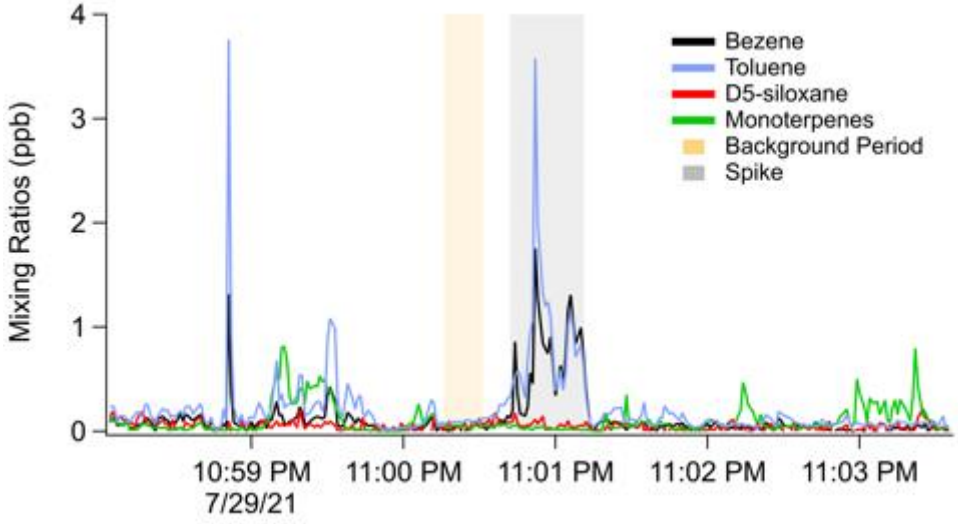

Figure S7. Mobile laboratory data showing the methods for screening for on-road mobile source emissions. Plumes are identified based on enhancements of aromatics and combustion tracers (not shown), and screened to exclude periods when VCP tracers, such as monoterpenes and D5-siloxane, are enhanced.

The resulting VOC profile is shown in Figure S8. The derived profile is very similar to the mobile fingerprint determined by Gkatzelis et al. (2021c). The profile demonstrates that ethanol is the dominant VOC from mobile sources measured by PTR-ToF-MS, followed by aromatics. Ethanol is also an important contributor to VCP emissions and therefore it is important to constrain ethanol for quantitatively apportioning VCP and mobile source emissions.

A series of sensitivity analyses were conducted to assess how the derived mobile source profile changes under different stringency criteria. Panels A, B, C, and D show sensitivity analyses when benzene is enhanced over background (BG) by varying amounts. Benzene enhancements above 2 ppb are considered "high emitters" and represent the upper 30% of all plumes identified in this analysis. Plumes averaged within the upper 74% of all emitters exhibit a similar mobile source profile as those averaged within the upper 94%. High emitters exhibit a significantly larger fraction of ethanol, but relatively similar proportion of aromatics. These results demonstrate that the fraction of ethanol in mobile source emission is likely between 0.5 – 0.6 ppb/ppb.

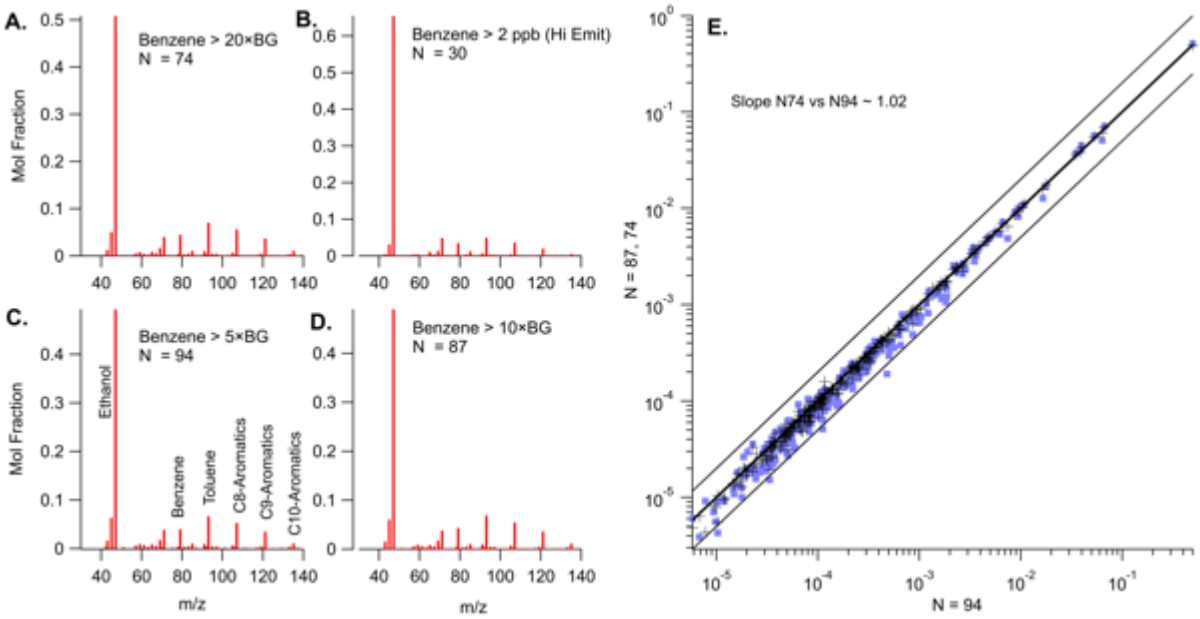

Figure S8. The derived mobile source profile based on mobile laboratory data screening processes shown in Figure 10. Panels A-D shows the derived profile under different stringency criteria, and panel E shows that screening the data to include the upper 74% of all plumes changes the derived mobile source profile by ~2 %.

5.2 PMF Results

Figures S9 and S10 show PMF results for 2 - 5 factor solutions. In all cases, the mobile source constraint is applied with an *a*-value = 0.75. Figure S11 shows the goodness-of-fit parameter, $Q/Q_{expected}$, which is the ratio of model residuals to the theoretical residuals expected for a data matrix fit to within experimental error. When $Q/Q_{expected} = 1$, the solution is considered well-fit. It is common to evaluate changes in $Q/Q_{expected}$ as additional factors are included.

For a two-factor solution, PMF attributes mass to a mobile source and all "other" sources (Figure S9). Pushing PMF to a three-factor solution results in split of the "other" category into a factor profile that peaks during the daytime, and another factor that is dominant at night. The daytime factor is primarily composed of oxygenated VOCs along with species known to be emitted or formed during daytime hours (e.g., biogenic VOCs like isoporene, methyl vinyl ketone +

methacrolein, and monoterpenes). Biogenic emissions in Las Vegas are very low (< 150 ppt, Coggon et al., 2023), therefore this daytime factor is primarily composed of oxidation products (Fig. S10). The nighttime factor is largely composed of VOCs linked to primary sources (e.g., VCPs and cooking), and its diurnal pattern is primarily driven by meteorology. The nocturnal boundary layer in Las Vegas is low, but daytime heat expands the boundary layer to as high as 10 km during the day (Langford et al., 2022).

When the solution is pushed to a four-factor solution, a factor is resolved that is primarily composed of toluene and acetone with smaller contributions from xylenes and parachlorobenzotriflouride (PCBTF). This factor exhibited a temporal profile characterized by brief, large enhancements in mixing ratios suggestive of a local source (Fig. 9, main text). PCBTF is a common component of solvent-borne coatings, such lacquers and paints (Stockwell et al., 2021), and we suspect that the source is associated with a cabinet-making shop located ~300 m from the Jerome Mack ground site. We do not consider this factor representative of the regional VOC mixtures and therefore do not analyze it further.

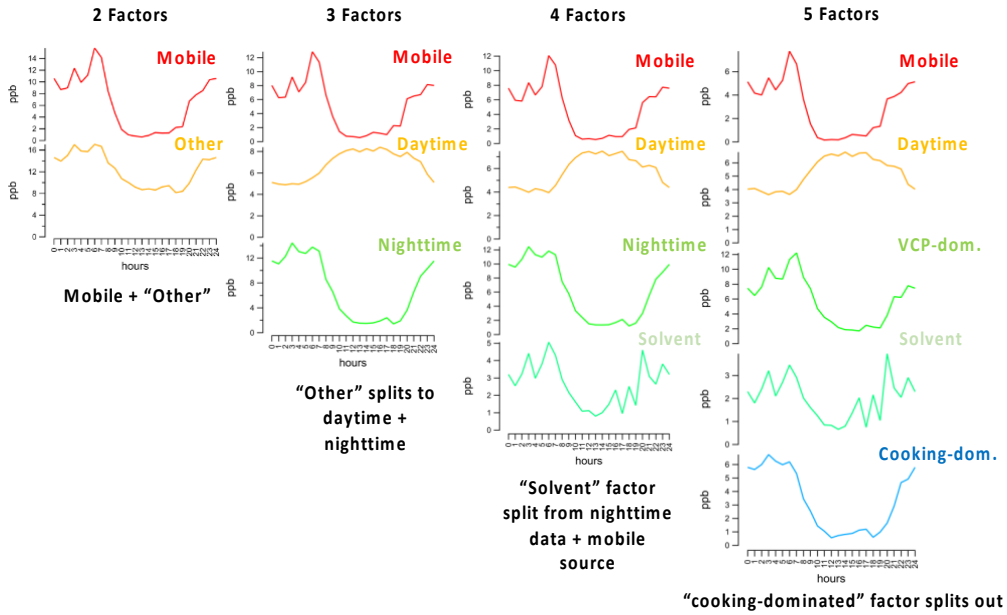

Figure S9. PMF diurnal profiles for 2 – 5 factors. Each column shows the resolved factor signal, and the description highlights the observed changes to the factor profiles.

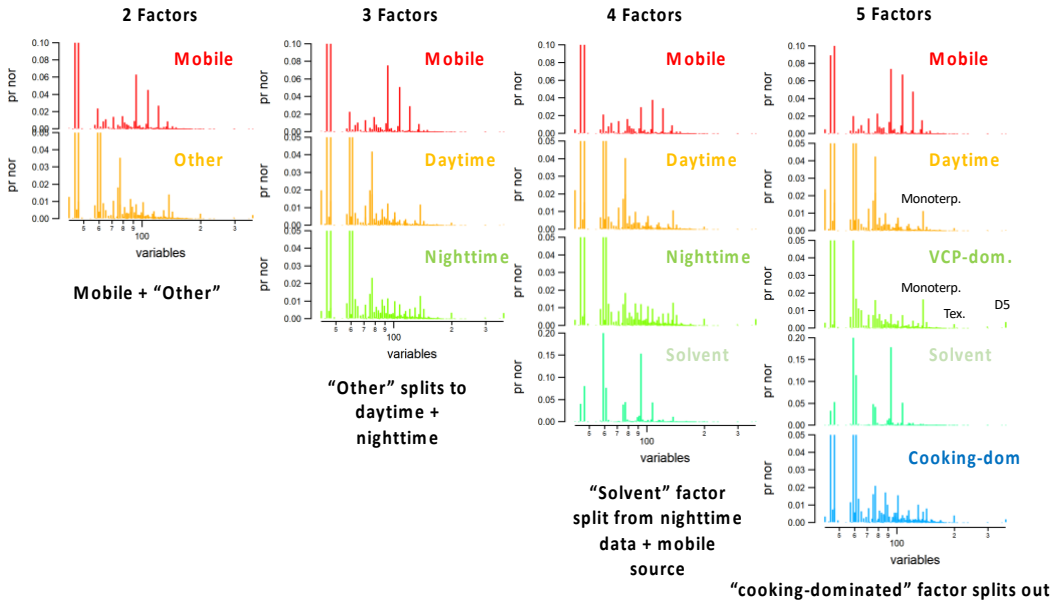

Figure S10. PMF factor profiles for 2 – 5 factors. Each column shows the resolved factor fingerprint, and the description highlights the observed changes to the factor profile.

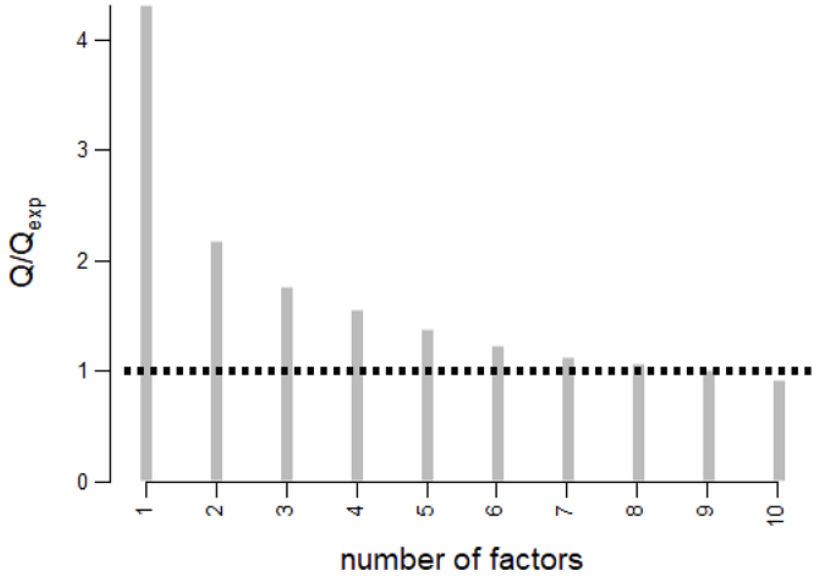

Figure S11. $Q/Q_{expected}$ for 1 – 10 factors. Increases to the factor profiles result in improved residuals

When the solution is finally pushed to five factors, PMF resolves a profile rich in aldehydes and another profile rich in ethanol, acetone, monoterpenes, and D5 These two factors are largely derived from the splitting of the nighttime and mobile source factors (Fig. S9). At 5 factors, the solution is nearly fit within the uncertainties of the measurements (Q/Q_{exp} = 1.3) and further increases in factors only result in modest improvements in residuals (Fig. S11).

The final two factors are consistent with the expected profiles for VCPs and cooking. The VCP-dominated factor is primarily composed of ethanol (EOH), but also contains D5-siloxane,

monoterpenes, and acetone, which are common ingredients in consumer products. This factor resembles the VCP-dominated factor resolved in the PMF analysis for NYC described by Gkatzelis et al. (2021b). In Section 4 of the main text, we show that the mass ratio of the VCP factor to the mobile source factor closely matches the distribution represented in emissions inventories for Clark County, NV (Fig. 11). The agreement between these distributions show that a five-factor solution reasonably explains the variability of important sources in the Las Vegas region. Solutions with a smaller number of factors overestimate the contribution of mobile source emissions, while solutions with larger numbers of factors do not provide meaningful factors.

The cooking-dominated factor contains the aldehyde and acids that are shown by mobile laboratory measurements to be associated with commercial cooking emissions in Las Vegas (see Section 3.2). Figure S12 demonstrates how the factor profile resolved by PMF compares against the cooking profile measured along the Las Vegas Strip. In general, the PMF profile closely resembles the cooking profile resolved from mobile laboratory drives. There are a number of masses resolved by PMF that were not identified by the correlation analysis (e.g. ethanol, acetaldehyde, and acetone + propanal). These VOCs have significant contributions from mobile source and VCP emissions and could not be attributed to cooking by the simple correlation analysis used to determine the cooking fingerprint along the Las Vegas Strip (see Section 3.2). There are also some masses which are apportioned at lower ratios, including nonanal and heptadienal. These masses are partially apportioned to the VCP factor. Likewise, masses typically attributed to VCPs are partially attributed to the cooking-dominated factor (e.g., siloxanes). The sharing of these "mixed" species between profiles reflects the uncertainties associated with apportioning VOCs from co-located sources. Despite these differences, the general agreement between the cooking-dominated factor and the profile determined from the Las Vegas Strip confirms that the five-factor solution effectively resolves the VOC mass associated with cooking activities. We note that the cooking-dominated profile, along with the other factors, resolved by PMF is provided in Table S1. Table S2 provides mass assignments to the cooking-dominated factor that could be used to speciate cooking profiles in inventories.

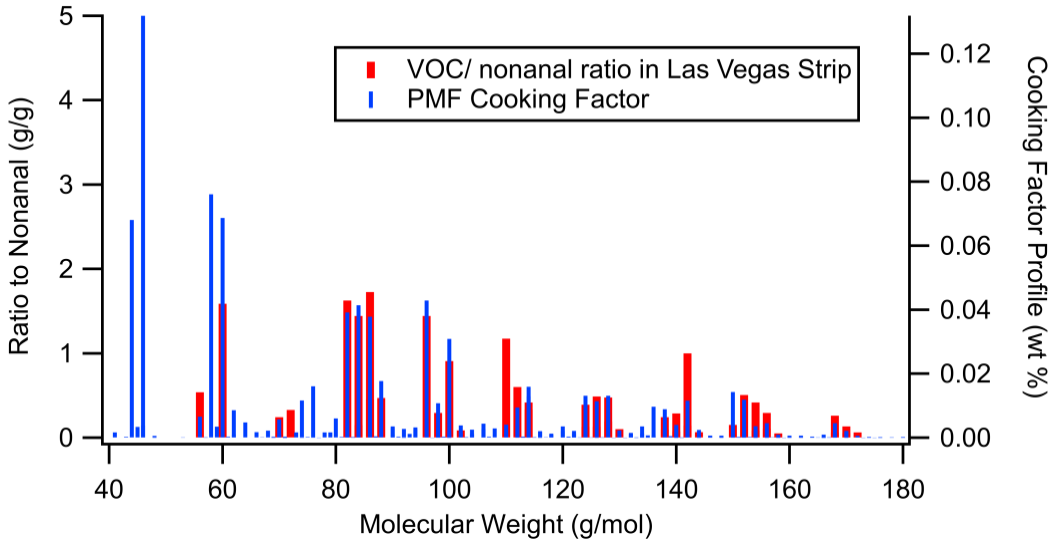

Figure S12. Comparison of the cooking-dominated factor resolved by PMF with the VOC/nonanal ratios observed along the Las Vegas Strip during mobile laboratory sampling.

Figure S13 shows how the 5-factor solution varies under different *a*-values applied to the mobile source constraint. With no constraint ($a = 1$), the mobile source factor is estimated to be ~2 times higher and the VCP-dominated factor ~4 times lower than what is resolved with more stringent constraints ($a < 1$). Similar observations were made by Gkatzelis et al. (2021b) and were associated with the overlap of VOCs that originate from both sources (e.g., ethanol, acetone, xylenes). The other factors (i.e., cooking-dominated, solvent, and daytime) show similar profiles as the solutions with $a < 1$. These results highlight the importance of applying source constraints in order to resolve VCP and mobile source emission contributions.

For solutions with $a < 1$, the profiles are similar though there is notable variability. We estimate the variability as the ratio between the standard deviation and mean calculated for all of the diurnal profiles with $a < 1$. On average, the mobile source and VCP profiles vary by 30% and 20%, respectively. This variability is reflected by changes to the PMF attribution of mass between these two sources. In contrast, the cooking-dominated, solvent, and daytime factors vary by < 7%. Consequently, while PMF variability may be highest for the mobile source and VCP factors, changes to the cooking-dominated factor are modest under different *a*-value constraints. In the main text, we present the solution for $a = 0.75$. This PMF analysis has the least constraints and provides a solution that best reflects the expected mobile source and VCP distribution represented by emissions inventories.

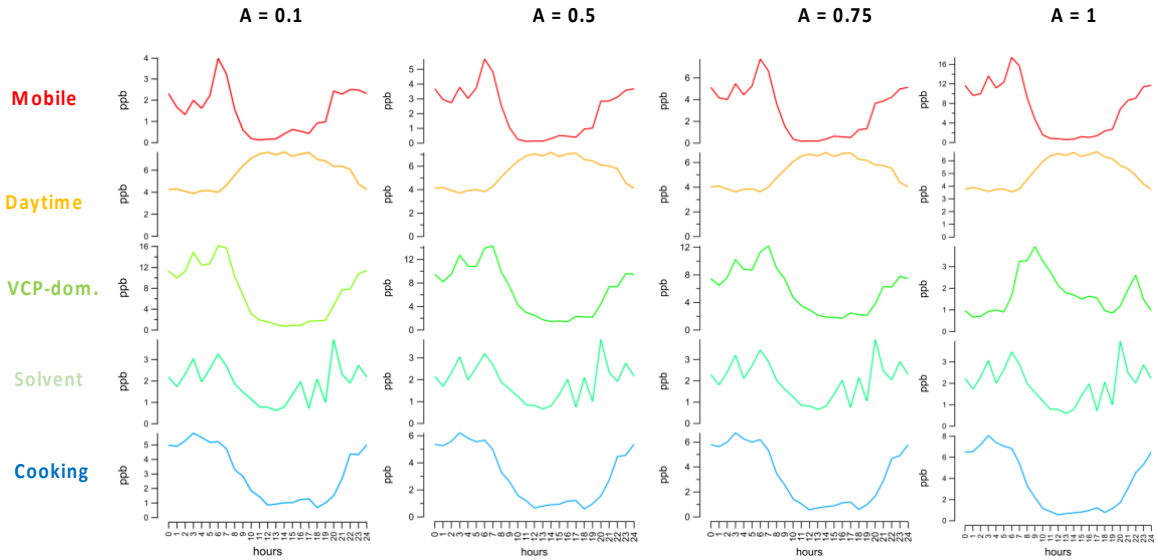

Figure S13. PMF solutions for a 5-factor system where the *a*-value applied to the mobile source constraint varies from 0.1 (highly constrained) to 1 (not constrained).

Table S1. PMF profiles (mass fraction) for the 5-factor solution presented in Fig. S10.

Ion	MW	Mobile Sources	VCP-dom.	Cooking-dom.	Chem.Ox. / Day Emiss.	Local Solvent
C2H3NH	42.034	0.003	0.002	0.002	0.015	0.000
HNCOH	44.013	0.000	0.000	0.000	0.001	0.000
C2H5NH	44.049	0.000	0.000	0.000	0.000	0.000
C2H4OH	45.033	0.059	0.114	0.068	0.057	0.033
CH3NOH	46.029	0.000	0.002	0.003	0.004	0.000
CH2O2H	47.013	0.000	0.003	0.004	0.012	0.001
C2H6OH	47.049	0.359	0.368	0.132	0.110	0.056
CH4SH	49.011	0.000	0.000	0.001	0.000	0.000
CH4O2H	49.028	0.000	0.000	0.000	0.000	0.000
C3H3NH	54.034	0.000	0.000	0.000	0.000	0.000
C3H4OH	57.033	0.003	0.006	0.007	0.006	0.002
C2H3NOH	58.029	0.000	0.000	0.000	0.000	0.000
C3H7NH	58.065	0.000	0.000	0.000	0.000	0.000
C3H6OH	59.049	0.018	0.129	0.076	0.299	0.371
C2H5NOH	60.044	0.000	0.000	0.003	0.005	0.000
C2H4O2H	61.028	0.002	0.015	0.069	0.109	0.115
CH3NO2H	62.024	0.000	0.000	0.000	0.000	0.000
C2H6SH	63.026	0.000	0.000	0.001	0.000	0.000
C2H6O2H	63.044	0.005	0.012	0.009	0.007	0.003
C2H8O2H	65.060	0.009	0.011	0.005	0.004	0.001
C5H6H	67.054	0.003	0.001	0.002	0.002	0.000
C4H5NH	68.049	0.000	0.000	0.000	0.000	0.000
C4H4OH	69.033	0.001	0.002	0.002	0.002	0.000
C3H3NOH	70.029	0.000	0.000	0.000	0.000	0.000
C4H7NH	70.065	0.000	0.000	0.000	0.000	0.000
C4H6OH	71.049	0.001	0.009	0.006	0.014	0.000
C5H10H	71.086	0.019	0.006	0.001	0.006	0.001
C2HNO2H	72.008	0.000	0.000	0.000	0.000	0.000
C3H5NOH	72.044	0.000	0.000	0.000	0.000	0.000
C4H8O	72.057	0.000	0.000	0.000	0.000	0.000
C4H9NH	72.081	0.000	0.000	0.000	0.000	0.000
C3H7NOH	74.060	0.000	0.000	0.002	0.001	0.000
C2H2O3H	75.008	0.000	0.000	0.000	0.000	0.000
C3H6O2H	75.044	0.001	0.009	0.012	0.021	0.047
C2H5NO2H	76.039	0.000	0.000	0.000	0.000	0.000
C2H4O3H	77.023	0.001	0.000	0.000	0.025	0.000

C3H8O2H	77.060	0.003	0.020	0.016	0.051	0.041
C5H3NH	78.034	0.000	0.000	0.000	0.000	0.000
C6H6H	79.054	0.027	0.007	0.002	0.005	0.005
C5H5NH	80.049	0.000	0.000	0.002	0.002	0.000
C6H8H	81.070	0.009	0.011	0.006	0.009	0.002
C5H7NH	82.065	0.000	0.000	0.000	0.000	0.000
C6H9H	82.078	0.000	0.000	0.000	0.000	0.000
CCl2H	82.945	0.000	0.001	0.001	0.000	0.000
C4H2O2H	83.013	0.000	0.000	0.000	0.001	0.000
C5H6OH	83.049	0.001	0.003	0.039	0.003	0.000
C6H10H	83.086	0.008	0.006	0.005	0.003	0.001
C4H5NOH	84.044	0.000	0.000	0.000	0.000	0.000
C5H8O	84.057	0.000	0.000	0.000	0.000	0.000
C5H9NH	84.081	0.000	0.000	0.000	0.000	0.000
C6H11H	84.093	0.000	0.000	0.000	0.000	0.000
C4H4O2H	85.028	0.000	0.001	0.004	0.005	0.000
C5H8OH	85.065	0.000	0.003	0.041	0.003	0.000
C6H12H	85.101	0.009	0.003	0.000	0.002	0.000
C4H6O2H	87.044	0.001	0.007	0.015	0.014	0.002
C5H10OH	87.080	0.001	0.007	0.038	0.005	0.001
C3H6NO2	88.039	0.000	0.000	0.000	0.000	0.000
C4H9NOH	88.076	0.000	0.000	0.000	0.000	0.000
C4H8O2H	89.060	0.000	0.005	0.018	0.005	0.011
C3H6O3H	91.039	0.000	0.001	0.001	0.005	0.000
C7H6H	91.054	0.017	0.001	0.003	0.000	0.015
C4H10O2H	91.075	0.001	0.004	0.003	0.006	0.004
C2H5NO3H	92.034	0.000	0.000	0.000	0.000	0.000
C7H8H	93.070	0.099	0.014	0.003	0.002	0.176
C4H12O2H	93.091	0.001	0.000	0.000	0.000	0.003
C6H7NH	94.065	0.000	0.000	0.001	0.000	0.000
C6H6OH	95.049	0.006	0.001	0.003	0.003	0.006
C7H10H	95.086	0.003	0.003	0.003	0.002	0.000
C5H4O2H	97.028	0.001	0.000	0.005	0.001	0.000
C6H8OH	97.065	0.001	0.002	0.043	0.002	0.000
C7H12H	97.101	0.008	0.004	0.003	0.002	0.001
C6H11NH	98.096	0.000	0.000	0.000	0.000	0.000
C4H2O3H	99.008	0.000	0.000	0.000	0.003	0.000
C5H6O2H	99.044	0.000	0.002	0.011	0.006	0.000
C6H10OH	99.080	0.001	0.003	0.003	0.002	0.001
C7H14H	99.117	0.000	0.000	0.000	0.000	0.000

C4H5NO2H	100.039	0.000	0.000	0.000	0.000	0.000
C5H9NOH	100.076	0.000	0.000	0.000	0.000	0.000
C4H4O3H	101.023	0.001	0.001	0.001	0.009	0.000
C5H8O2H	101.060	0.001	0.007	0.031	0.012	0.005
C6H12OH	101.096	0.002	0.003	0.002	0.001	0.002
C7H16H	101.132	0.000	0.000	0.000	0.000	0.000
C4H6O3H	103.039	0.000	0.001	0.002	0.003	0.000
C5H10O2H	103.075	0.000	0.001	0.004	0.001	0.000
C7H5NH	104.049	0.000	0.000	0.000	0.000	0.000
C4H9NO2H	104.071	0.000	0.000	0.000	0.000	0.000
C4H8O3H	105.055	0.000	0.001	0.002	0.004	0.000
C8H8H	105.070	0.015	0.000	0.001	0.000	0.005
C5H12O2H	105.091	0.000	0.002	0.001	0.002	0.000
C7H6OH	107.049	0.001	0.003	0.004	0.001	0.000
C4H10O3H	107.070	0.000	0.000	0.000	0.001	0.001
C8H10H	107.086	0.106	0.014	0.003	0.000	0.051
C6H5NOH	108.044	0.000	0.000	0.000	0.000	0.000
C8H12H	109.101	0.002	0.002	0.003	0.001	0.000
C7H10OH	111.080	0.000	0.003	0.004	0.000	0.000
C8H14H	111.117	0.004	0.002	0.002	0.001	0.000
C6H8O2H	113.060	0.001	0.003	0.004	0.005	0.000
C7H12OH	113.096	0.000	0.001	0.009	0.001	0.000
C8H16H	113.132	0.000	0.000	0.000	0.000	0.000
C4H3NO3H	114.019	0.000	0.000	0.000	0.000	0.000
C5H7NO2H	114.055	0.000	0.000	0.000	0.000	0.000
C6H11NOH	114.091	0.000	0.000	0.000	0.000	0.000
C5H6O3H	115.039	0.000	0.001	0.002	0.002	0.000
C6H10O2H	115.075	0.000	0.004	0.016	0.007	0.000
C7H14OH	115.112	0.000	0.001	0.013	0.000	0.005
C8H18H	115.148	0.000	0.000	0.000	0.000	0.000
C5H9NO2H	116.071	0.000	0.000	0.000	0.000	0.000
C6H13NOH	116.107	0.000	0.000	0.000	0.000	0.000
C5H8O3H	117.055	0.000	0.001	0.002	0.003	0.000
C9H8H	117.070	0.001	0.000	0.000	0.000	0.000
C6H12O2H	117.091	0.000	0.001	0.002	0.001	0.004
C4H7NO3H	118.050	0.000	0.000	0.000	0.000	0.000
C5H10O3H	119.070	0.000	0.001	0.001	0.001	0.000
C9H10H	119.086	0.007	0.000	0.001	0.001	0.000
C6H14O2H	119.107	0.001	0.002	0.001	0.000	0.001
C4H8O4H	121.050	0.001	0.000	0.000	0.001	0.000

C8H8OH	121.065	0.001	0.002	0.002	0.001	0.000
C9H12H	121.101	0.087	0.010	0.003	0.000	0.005
C3H7NO4H	122.045	0.000	0.000	0.000	0.000	0.000
C7H7NOH	122.060	0.000	0.000	0.000	0.000	0.000
C8H11NH	122.096	0.000	0.000	0.000	0.000	0.000
C7H6O2H	123.044	0.000	0.000	0.001	0.001	0.000
C4H10O4H	123.065	0.000	0.000	0.000	0.001	0.000
C8H10OH	123.080	0.000	0.000	0.000	0.000	0.000
C9H14H	123.117	0.001	0.002	0.002	0.000	0.000
C6H5NO2H	124.039	0.000	0.000	0.000	0.000	0.000
C7H8O2H	125.060	0.000	0.002	0.005	0.002	0.000
C8H12OH	125.096	0.000	0.001	0.013	0.001	0.000
C9H16H	125.132	0.002	0.001	0.001	0.000	0.000
C7H11NOH	126.091	0.000	0.000	0.000	0.000	0.000
C7H10O2H	127.075	0.000	0.002	0.000	0.000	0.000
C8H14OH	127.112	0.000	0.001	0.011	0.001	0.000
C6H9NO2H	128.071	0.000	0.000	0.000	0.000	0.000
C7H13NOH	128.107	0.000	0.000	0.000	0.000	0.000
C7H12O2H	129.091	0.000	0.002	0.008	0.002	0.000
C8H16OH	129.127	0.002	0.006	0.013	0.005	0.001
C4H3NO4H	130.013	0.000	0.000	0.000	0.000	0.000
C6H10O3H	131.070	0.001	0.001	0.002	0.003	0.000
C7H14O2H	131.107	0.000	0.001	0.001	0.000	0.000
C4H5NO4H	132.029	0.000	0.000	0.000	0.000	0.000
C5H8O4H	133.050	0.000	0.000	0.001	0.002	0.000
C6H12O3H	133.086	0.000	0.000	0.001	0.001	0.002
C10H12H	133.101	0.009	0.001	0.001	0.001	0.000
C7H16O2H	133.122	0.000	0.000	0.001	0.000	0.002
C10H14	134.109	0.001	0.000	0.000	0.000	0.000
C6H15NO2H	134.118	0.000	0.000	0.000	0.000	0.000
C4H6O5H	135.029	0.000	0.000	0.000	0.001	0.000
C8H6O2H	135.044	0.000	0.000	0.000	0.000	0.000
C9H10OH	135.080	0.001	0.000	0.001	0.000	0.000
C10H14H	135.117	0.031	0.003	0.003	0.000	0.000
C7H5NSH	136.022	0.002	0.002	0.001	0.001	0.000
C8H9NOH	136.076	0.000	0.000	0.000	0.000	0.000
C4H8O5H	137.044	0.000	0.000	0.000	0.001	0.000
C8H8O2H	137.060	0.000	0.000	0.001	0.000	0.000
C9H12OH	137.096	0.000	0.000	0.000	0.000	0.000
C10H16H	137.132	0.000	0.037	0.010	0.023	0.003

C8H10O2H	139.075	0.000	0.001	0.003	0.001	0.000
C9H14OH	139.112	0.000	0.000	0.009	0.001	0.000
C10H18H	139.148	0.000	0.000	0.000	0.000	0.000
C6H5NO3H	140.034	0.000	0.000	0.000	0.000	0.000
C6H4O4H	141.018	0.000	0.000	0.000	0.001	0.000
C7H8O3H	141.055	0.000	0.000	0.001	0.001	0.000
C8H12O2H	141.091	0.000	0.000	0.003	0.001	0.000
C9H16OH	141.127	0.000	0.001	0.004	0.001	0.000
C10H20H	141.164	0.000	0.000	0.000	0.000	0.000
C5H3NO4H	142.013	0.000	0.000	0.000	0.000	0.000
C6H7NO3H	142.050	0.000	0.000	0.000	0.000	0.000
C6H6O4H	143.034	0.000	0.000	0.000	0.001	0.000
C7H10O3H	143.070	0.000	0.001	0.000	0.001	0.000
C11H10H	143.086	0.004	0.000	0.001	0.000	0.000
C8H14O2H	143.107	0.000	0.001	0.006	0.001	0.000
C9H18OH	143.143	0.004	0.008	0.012	0.005	0.001
C5H4O5H	145.013	0.000	0.000	0.000	0.000	0.000
C6H8O4H	145.050	0.000	0.000	0.001	0.001	0.000
C7H12O3H	145.086	0.000	0.000	0.000	0.000	0.000
C8H16O2H	145.122	0.000	0.000	0.002	0.000	0.000
C6H4Cl2H	146.976	0.000	0.002	0.000	0.000	0.000
C5H6O5H	147.029	0.000	0.000	0.000	0.000	0.000
C6H10O4H	147.065	0.000	0.000	0.000	0.001	0.000
C7H14O3H	147.102	0.000	0.000	0.001	0.000	0.000
C8H18O2H	147.138	0.000	0.000	0.001	0.000	0.000
C8H4O3H	149.023	0.000	0.000	0.000	0.002	0.000
C9H8O2H	149.060	0.000	0.000	0.000	0.000	0.000
C6H12O4H	149.081	0.000	0.000	0.000	0.000	0.000
C10H12OH	149.096	0.001	0.000	0.001	0.000	0.000
C11H16H	149.132	0.007	0.001	0.001	0.000	0.000
C9H10O2H	151.075	0.000	0.000	0.000	0.000	0.000
C10H14OH	151.112	0.000	0.001	0.014	0.000	0.000
C11H18H	151.148	0.000	0.001	0.000	0.000	0.000
C9H13NOH	152.107	0.000	0.000	0.000	0.000	0.000
C10H17NH	152.143	0.000	0.000	0.000	0.000	0.000
C8H8O3H	153.055	0.000	0.000	0.001	0.000	0.000
C9H12O2H	153.091	0.000	0.001	0.001	0.000	0.000
C10H16OH	153.127	0.000	0.000	0.012	0.000	0.000
C11H20H	153.164	0.000	0.000	0.000	0.000	0.000
C7H7NO3H	154.050	0.000	0.000	0.000	0.000	0.000

C7H6O4H	155.034	0.000	0.000	0.000	0.000	0.000
C8H10O3H	155.070	0.000	0.000	0.000	0.000	0.000
C9H14O2H	155.107	0.000	0.000	0.002	0.001	0.000
C10H18OH	155.143	0.000	0.000	0.004	0.000	0.000
C11H22H	155.179	0.000	0.000	0.000	0.000	0.000
C6H4O5H	157.013	0.000	0.000	0.000	0.000	0.000
C7H8O4H	157.050	0.000	0.000	0.000	0.001	0.000
C8H12O3H	157.086	0.000	0.000	0.000	0.000	0.000
C9H16O2H	157.122	0.000	0.000	0.002	0.001	0.000
C10H20OH	157.159	0.000	0.000	0.004	0.000	0.000
C6H7NO4H	158.045	0.000	0.000	0.000	0.000	0.000
C6H6O5H	159.029	0.000	0.000	0.000	0.001	0.000
C7H10O4H	159.065	0.000	0.000	0.000	0.001	0.000
C8H14O3H	159.102	0.000	0.000	0.000	0.000	0.000
C12H14H	159.117	0.000	0.000	0.000	0.000	0.000
C9H18O2H	159.138	0.000	0.000	0.001	0.000	0.000
C6H9NO4H	160.060	0.000	0.000	0.000	0.000	0.000
C7H3ClF2H	160.996	0.000	0.002	0.000	0.001	0.001
C7H12O4H	161.081	0.000	0.000	0.000	0.000	0.000
C11H12OH	161.096	0.000	0.000	0.000	0.000	0.000
C9H20O2H	161.154	0.000	0.000	0.001	0.000	0.000
C9H6O3H	163.039	0.000	0.000	0.000	0.001	0.000
C10H10O2H	163.075	0.000	0.000	0.000	0.000	0.000
C8H18O3H	163.133	0.000	0.000	0.001	0.000	0.000
C12H18H	163.148	0.002	0.000	0.000	0.000	0.000
C10H12O2H	165.091	0.000	0.000	0.000	0.000	0.000
C7H16O4H	165.112	0.000	0.000	0.000	0.000	0.000
C11H16OH	165.127	0.000	0.000	0.000	0.000	0.000
C12H20H	165.164	0.000	0.000	0.000	0.000	0.000
C8H7NO3H	166.050	0.000	0.000	0.000	0.000	0.000
C8H6O4H	167.034	0.000	0.000	0.000	0.002	0.000
C9H10O3H	167.070	0.000	0.000	0.000	0.000	0.000
C10H14O2H	167.107	0.000	0.000	0.001	0.000	0.000
C11H18OH	167.143	0.000	0.000	0.000	0.000	0.000
C12H22H	167.179	0.000	0.000	0.000	0.000	0.000
C8H9NO3H	168.066	0.000	0.000	0.000	0.000	0.000
C9H13NO2H	168.102	0.000	0.000	0.000	0.000	0.000
C8H8O4H	169.050	0.000	0.000	0.000	0.000	0.000
C9H12O3H	169.086	0.000	0.000	0.000	0.000	0.000
C10H16O2H	169.122	0.000	0.001	0.004	0.000	0.000

C11H20OH	169.159	0.000	0.000	0.001	0.000	0.000
C12H24H	169.195	0.000	0.000	0.000	0.000	0.000
C7H6O5H	171.029	0.000	0.000	0.000	0.000	0.000
C10H18O2H	171.138	0.000	0.000	0.002	0.000	0.000
C11H22OH	171.174	0.000	0.000	0.002	0.000	0.000
C9H16O3H	173.117	0.000	0.000	0.000	0.000	0.000
C10H20O2H	173.154	0.000	0.000	0.001	0.000	0.000
C7H11NO4H	174.076	0.000	0.000	0.000	0.000	0.000
C6H6O6H	175.024	0.000	0.000	0.000	0.000	0.000
C13H18H	175.148	0.001	0.000	0.000	0.000	0.000
C10H22O2H	175.169	0.000	0.000	0.000	0.000	0.000
C6H9NO5H	176.055	0.000	0.000	0.000	0.000	0.000
C6H8O6H	177.039	0.000	0.000	0.000	0.000	0.000
C7H12O5H	177.076	0.000	0.000	0.000	0.000	0.000
C9H20O3H	177.149	0.000	0.000	0.000	0.000	0.000
C13H20H	177.164	0.001	0.000	0.000	0.000	0.000
C11H14O2H	179.107	0.000	0.000	0.000	0.000	0.000
C13H22H	179.179	0.000	0.000	0.000	0.000	0.000
C12H20OH	181.159	0.000	0.000	0.000	0.000	0.000
C13H24H	181.195	0.000	0.000	0.000	0.000	0.000
C13H14OH	187.112	0.000	0.000	0.000	0.000	0.000
C14H18H	187.148	0.000	0.000	0.000	0.000	0.000
C14H20H	189.164	0.000	0.000	0.000	0.000	0.000
C14H24H	193.195	0.000	0.000	0.000	0.000	0.000
C14H26H	195.211	0.000	0.000	0.000	0.000	0.000
C14H28H	197.226	0.000	0.000	0.000	0.000	0.000
C12H22O2H	199.169	0.000	0.008	0.008	0.004	0.000
C13H26OH	199.206	0.000	0.000	0.002	0.000	0.000
C14H16OH	201.127	0.000	0.000	0.000	0.000	0.000
C15H25	205.195	0.000	0.000	0.000	0.000	0.000
C14H22OH	207.174	0.000	0.000	0.000	0.000	0.000
C15H26H	207.211	0.000	0.000	0.000	0.000	0.000
C10H24O3SiH	221.157	0.000	0.000	0.000	0.000	0.000
C10H8O6H	225.039	0.000	0.000	0.000	0.000	0.000
C17H28H	233.226	0.000	0.000	0.000	0.000	0.000
C16H26OH	235.206	0.000	0.000	0.000	0.000	0.000
C8H24O4Si4H	297.082	0.000	0.004	0.001	0.000	0.000
C7H20O4Si4H2OH	299.062	0.000	0.000	0.000	0.000	0.000
C9H26Si5O5H	355.070	0.000	0.001	0.000	0.000	0.000
C10H30O5Si5H	371.102	0.000	0.021	0.008	0.000	0.000

Table S2. Cooking-dominated profile resolved by PMF with species assignments based on the GC measurements described by Klein et al. (2016). The "Unspeciated" fraction reflects the total mass resolved by PMF that is not assigned to a specific isomer or molecular functionality (e.g., aldehyde or acid). This fraction also includes masses that were attributed to the cooking-dominated factor but are more likely associated with co-located sources, such as VCPs (e.g., siloxanes). These "mixed" masses shared between factors represent < 2% of the total mass.

Assigned Species	Formula	SMILES	MW (g/mol)	Class	Mass Fraction	Notes
acetaldehyde	C2H4O	CC=O	44.05	Ald	0.069	a,c
ethanol	C2H6O	CCO	46.07	Alc	0.132	a,c
acrolein	C3H4O	C=CC=O	56.06	Ald	0.007	a,c
propanal	C3H6O	CCC=O	58.08	Ald	0.076	a,c
acetic acid	C2H4O2	CC(O)=O	60.05	Acid	0.069	a,c
butenal	C4H6O	CC=CC=O	70.09	Ald	0.006	a,c
propanoic acid	C3H6O2	CCC(=O)O	74.08	Acid	0.012	a,c
pentadienal	C5H6O	C=CC=CC=O	82.1	Ald	0.039	a,c
butenedial	C4H4O2	C(=CC=O)C=O	84.07	Ald	0.004	a,c
pentenal	C5H10O	CCC=CC=O	84.12	Ald	0.041	a,c
pentanal	C5H10O	CCCCC=O	86.13	Ald	0.038	a,c
butyrolactone	C4H6O2	O=C1OCCC1	86.09	Ket	0.015	a,c
hexadienal	C6H8O	CC=CC=CC=O	96.13	Ald	0.043	a,c
pentanoic acid	C5H10O2	CCCCC(=O)O	102.13	Acid	0.004	a,c
heptadienal	C7H10O	CCC=CC=CC=O	110.15	Ald	0.004	a,c
heptenal	C7H12O	CCCCC=CC=O	112.17	Ald	0.009	a,c
heptanal	C7H14O	CCCCCCC=O	114.19	Ald	0.013	a,c
octadienal	C8H12O	CCCC=CC=CC=O	124.18	Ald	0.013	a,c
octenal	C8H14O	CCCCCC=CC=O	126.2	Ald	0.011	a,c
octanal	C8H16O	CCCCCCCC=O	128.21	Ald	0.013	a,c
heptanoic acid	C7H14O2	CCCCCCC(=O)O	130.18	Acid	0.001	a,c
monoterpene	C10H16	---	136.23	Terp	0.010	a,c
nonadienal	C9H14O	CCCCC=CC=CC=O	138.21	Ald	0.009	a,c
nonenal	C9H16O	CCCCCCC=CC=O	140.22	Ald	0.004	a,c
nonanal	C9H18O	CCCCCCCCC=O	142.24	Ald	0.012	a,c
octanoic acid	C8H16O2	CCCCCCCC(=O)O	144.21	Acid	0.002	a,c
decatrienal	C10H14O	CCCC=CC=CC=CC=O	150.22	Ald	0.014	b,c
decadienal	C10H16O	CCCCCC=CC=CC=O	152.23	Ald	0.012	a,c
decenal	C10H18O	CCCCCCCC=CC=O	154.25	Ald	0.004	a,c
decanal	C10H20O	CCCCCCCCCC=O	156.26	Ald	0.004	a,c
nonanoic acid	C9H18O2	CCCCCCCCC(=O)O	158.24	Acid	0.001	a,c
undecenal	C11H22O	CCCCCCCCC=CC=O	168.28	Ald	0.001	a,c
undecanal	C11H20O	CCCCCCCCCC=O	170.29	Ald	0.002	a,c
decenoic acid	C10H18O2	CCCCCCCC=CC(=O)O	170.25	Acid	0.002	b,c
decanoic acid	C10H20O2	CCCCCCCCCC(=O)O	172.26	Acid	0.001	a,c
tridecanal	C13H26O	CCCCCCCCCCCCC=O	198.34	Ald	0.002	a,c
Total Assigned Masses					***0.70***	

Other Masses (lower certainty)						
furfural	C5H4O2	C1=COC(=C1)C=O	96.08	Ald	0.005	b,c
C7H8O2	C7H8O2	---	124.14	Acid	0.005	c
benzaldehyde	C7H6O	C1=CC=C(C=C1)C=O	106.12	Ald	0.004	a,c
C6H8O2	C6H8O2	---	112.13	Acid	0.004	c
C6H10O2	C6H10O2	---	114.14	Acid	0.016	c
C8H10O2	C8H10O2	---	138.16	Acid	0.003	c
C8H12O2	C8H12O2	---	140.18	Acid	0.003	c
C8H14O2	C8H14O2	---	142.2	Acid	0.006	c
C9H14O2	C9H14O2	---	154.21	Acid	0.002	c
C9H16O2	C9H16O2	---	156.22	Acid	0.002	c
Total Other Masses					***0.05***	
Unspeciated					***0.25***	

[a] isomer identity based on identity reported by Klein et al. (2016)
[b] assumed isomer identity
[c] compound class based on assignments given by Klein et al. (2016)

References

Bishop, G. A., and Haugen, M. J.: The Story of Ever Diminishing Vehicle Tailpipe Emissions as Observed in the Chicago, Illinois Area, Environ. Sci. Technol., 52, 7587-7593, 10.1021/acs.est.8b00926, 2018.

Buhr, K., van Ruth, S., and Delahunty, C.: Analysis of volatile flavour compounds by Proton Transfer Reaction-Mass Spectrometry: fragmentation patterns and discrimination between isobaric and isomeric compounds, International Journal of Mass Spectrometry, 221, 1-7, https://doi.org/10.1016/S1387-3806(02)00896-5, 2002.

Canonaco, F., Crippa, M., Slowik, J. G., Baltensperger, U., and Prévôt, A. S. H.: SoFi, an IGOR-based interface for the efficient use of the generalized multilinear engine (ME-2) for the source apportionment: ME-2 application to aerosol mass spectrometer data, Atmos. Meas. Tech., 6, 3649-3661, 10.5194/amt-6-3649-2013, 2013.

Coggon, M. M., Stockwell, C. E., Claflin, M. S., Pfannerstill, E. Y., Lu, X., Gilman, J. B., Marcantonio, J., Cao, C., Bates, K., Gkatzelis, G. I., Lamplugh, A., Katz, E. F., Arata, C., Apel, E. C., Hornbrook, R. S., Piel, F., Majluf, F., Blake, D. R., Wisthaler, A., Canagaratna, M., Lerner, B. M., Goldstein, A. H., Mak, J. E., and Warneke, C.: Identifying and correcting interferences to PTR-ToF-MS measurements of isoprene and other urban volatile organic compounds, EGUsphere, 2023, 1-41, 10.5194/egusphere-2023-1497, 2023.

Gkatzelis, G. I., Coggon, M. M., McDonald, B. C., Peischl, J., Aikin, K. C., Gilman, J. B., Trainer, M., and Warneke, C.: Identifying Volatile Chemical Product Tracer Compounds in US Cities, Environ. Sci. Technol., 55, 188-199, 10.1021/acs.est.0c05467, 2021a.

Gkatzelis, G. I., Coggon, M. M., McDonald, B. C., Peischl, J., Gilman, J. B., Aikin, K. C., Robinson, M. A., Canonaco, F., Prevot, A. S. H., Trainer, M., and Warneke, C.: Observations

Confirm that Volatile Chemical Products Are a Major Source of Petrochemical Emissions in U.S. Cities, Environmental Science & Technology, 55, 4332-4343, 10.1021/acs.est.0c05471, 2021b.

Gkatzelis, G. I., Coggon, M. M., McDonald, B. C., Peischl, J., Gilman, J. B., Aikin, K. C., Robinson, M. A., Canonaco, F., Prevot, A. S. H., Trainer, M., and Warneke, C.: Observations Confirm that Volatile Chemical Products Are a Major Source of Petrochemical Emissions in US Cities, Environ. Sci. Technol., 55, 4332-4343, 10.1021/acs.est.0c05471, 2021c.

Gueneron, M., Erickson, M. H., VanderSchelden, G. S., and Jobson, B. T.: PTR-MS fragmentation patterns of gasoline hydrocarbons, International Journal of Mass Spectrometry, 379, 97-109, https://doi.org/10.1016/j.ijms.2015.01.001, 2015.

Klein, F., Platt, S. M., Farren, N. J., Detournay, A., Bruns, E. A., Bozzetti, C., Daellenbach, K. R., Kilic, D., Kumar, N. K., Pieber, S. M., Slowik, J. G., Temime-Roussel, B., Marchand, N., Hamilton, J. F., Baltensperger, U., Prévôt, A. S. H., and El Haddad, I.: Characterization of Gas-Phase Organics Using Proton Transfer Reaction Time-of-Flight Mass Spectrometry: Cooking Emissions, Environmental Science & Technology, 50, 1243-1250, 10.1021/acs.est.5b04618, 2016.

Langford, A. O., Senff, C. J., Alvarez Ii, R. J., Aikin, K. C., Baidar, S., Bonin, T. A., Brewer, W. A., Brioude, J., Brown, S. S., Burley, J. D., Caputi, D. J., Conley, S. A., Cullis, P. D., Decker, Z. C. J., Evan, S., Kirgis, G., Lin, M., Pagowski, M., Peischl, J., Petropavlovskikh, I., Pierce, R. B., Ryerson, T. B., Sandberg, S. P., Sterling, C. W., Weickmann, A. M., and Zhang, L.: The Fires, Asian, and Stratospheric Transport–Las Vegas Ozone Study (FAST-LVOS), Atmos. Chem. Phys., 22, 1707-1737, 10.5194/acp-22-1707-2022, 2022.

McDonald, B. C., de Gouw, J. A., Gilman, J. B., Jathar, S. H., Akherati, A., Cappa, C. D., Jimenez, J. L., Lee-Taylor, J., Hayes, P. L., McKeen, S. A., Cui, Y. Y., Kim, S. W., Gentner, D. R., Isaacman-VanWertz, G., Goldstein, A. H., Harley, R. A., Frost, G. J., Roberts, J. M., Ryerson, T. B., and Trainer, M.: Volatile chemical products emerging as largest petrochemical source of urban organic emissions, Science, 359, 760-764, 10.1126/science.aaq0524, 2018.

Paatero, P.: The Multilinear Engine—A Table-Driven, Least Squares Program for Solving Multilinear Problems, Including the n-Way Parallel Factor Analysis Model, Journal of Computational and Graphical Statistics, 8, 854-888, 10.1080/10618600.1999.10474853, 1999.

Pagonis, D., Sekimoto, K., and de Gouw, J.: A Library of Proton-Transfer Reactions of H3O+ Ions Used for Trace Gas Detection, Journal of The American Society for Mass Spectrometry, 30, 1330-1335, 10.1007/s13361-019-02209-3, 2019.

Schauer, J. J., Kleeman, M. J., Cass, G. R., and Simoneit, B. R. T.: Measurement of Emissions from Air Pollution Sources. 1. C1 through C29 Organic Compounds from Meat Charbroiling, Environmental Science & Technology, 33, 1566-1577, 10.1021/es980076j, 1999.

Sekimoto, K., Li, S.-M., Yuan, B., Koss, A., Coggon, M., Warneke, C., and de Gouw, J.: Calculation of the sensitivity of proton-transfer-reaction mass spectrometry (PTR-MS) for organic trace gases using molecular properties, International Journal of Mass Spectrometry, 421, 71-94, https://doi.org/10.1016/j.ijms.2017.04.006, 2017.

Restaurant Inspections from the Southern Nevada Health District (SNHD). https://opendataportal-lasvegas.opendata.arcgis.com/datasets/restaurant-inspections-open-data/explore, access: December 28, 2021, 2021.

Stockwell, C. E., Coggon, M. M., Gkatzelis, G. I., Ortega, J., McDonald, B. C., Peischl, J., Aikin, K., Gilman, J. B., Trainer, M., and Warneke, C.: Volatile organic compound emissions from solvent- and water-borne coatings – compositional differences and tracer compound identifications, Atmos. Chem. Phys., 21, 6005-6022, 10.5194/acp-21-6005-2021, 2021.

Ulbrich, I. M., Canagaratna, M. R., Zhang, Q., Worsnop, D. R., and Jimenez, J. L.: Interpretation of organic components from Positive Matrix Factorization of aerosol mass spectrometric data, Atmos. Chem. Phys., 9, 2891-2918, 10.5194/acp-9-2891-2009, 2009.

Warneke, C., de Gouw, J. A., Holloway, J. S., Peischl, J., Ryerson, T. B., Atlas, E., Blake, D., Trainer, M., and Parrish, D. D.: Multiyear trends in volatile organic compounds in Los Angeles, California: Five decades of decreasing emissions, J. Geophs. Res., 117, 1-10, 10.1029/2012jd017899, 2012.

Warneke, C., Geiger, F., Edwards, P. M., Dube, W., Pétron, G., Kofler, J., Zahn, A., Brown, S. S., Graus, M., Gilman, J. B., Lerner, B. M., Peischl, J., Ryerson, T. B., de Gouw, J. A., and Roberts, J. M.: Volatile organic compound emissions from the oil and natural gas industry in the Uintah Basin, Utah: oil and gas well pad emissions compared to ambient air composition, Atmos. Chem. Phys., 14, 10977-10988, 10.5194/acp-14-10977-2014, 2014.